UCRL- 100984
PREPRINT

THE INTERACTION OF SUPERNOVAE WITH CIRCUMSTELLAR BUBBLES

Roger A. Chevalier
Department of Astronomy
University of Virginia
and
Edison P. Liang
Physics Department
Lawrence Livermore National Laboratory
University of California

This paper was prepared for submittal to
Astrophysics Journal

May 1989

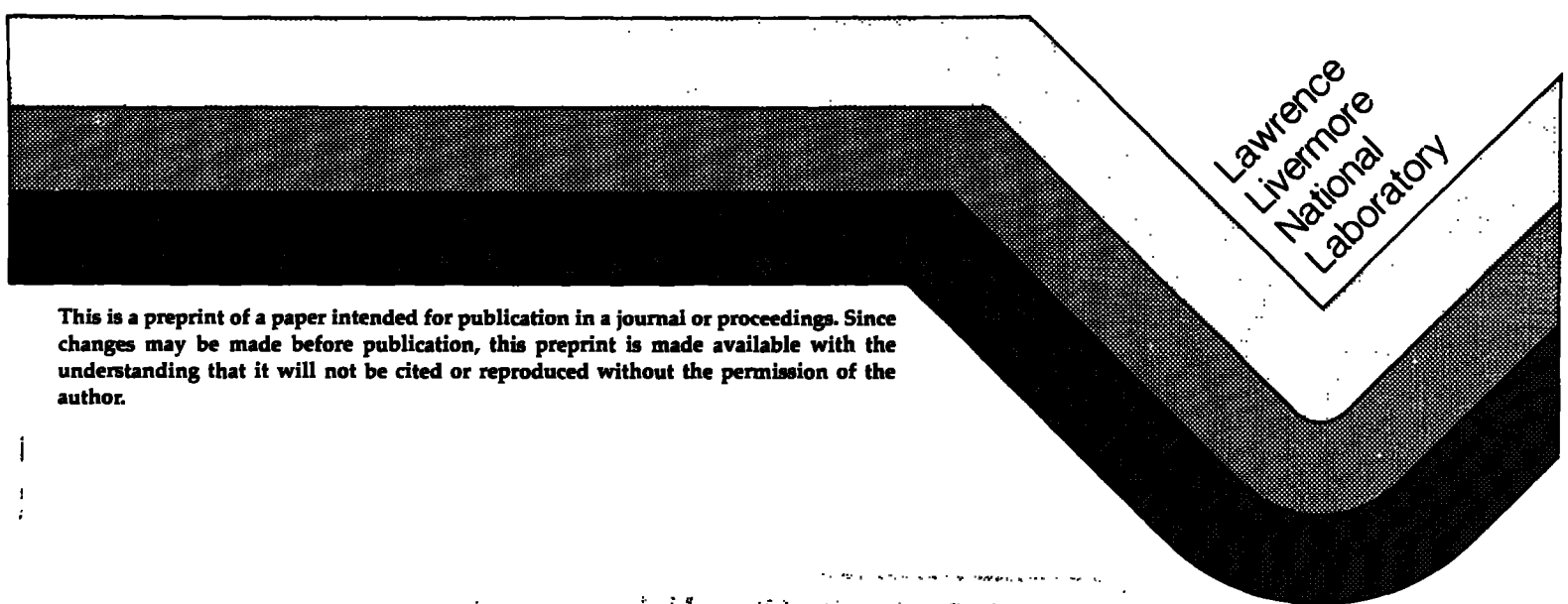

THE INTERACTION OF SUPERNOVAE WITH CIRCUMSTELLAR BUBBLES

Roger A. Chevalier

Department of Astronomy

University of Virginia

and

Edison P. Liang

Physics Department

Lawrence Livermore National Laboratory

University of California

ABSTRACT

The fast winds from blue massive star can create low density bubbles that are surrounded by shells. When the massive star explodes at the end of its life, it freely expands into the low density bubble, with an outer shock interaction region. The initial interaction with the dense shell creates a reflected shock in the interaction region and begins to drive a shock wave in the shell. The pressure of the shocked supernova gas rises as the steep outer density profile of the supernova interacts with the shell. Both the structure of the shocked supernova gas and the shock propagation into the shell can be described by self-similar solutions. The pressure in the shocked gas interaction region begins to decline when either the flat portion of the supernova density profile reaches the shell, the energy transfer to the shell is significant, or the outer shock wave traverses the shell. Typically, we find that the shock traversal occurs before the energy transfer is significant. The supernova remnant Cas A is probably a good example of compact shell interaction. Our model predicts that the bright X-ray and radio ring is shocked dense wind gas, and hot, shocked supernova gas is inside of the ring. Compact radio sources observed in NGC 4449 and in the starburst nuclei of M82 and NGC 253 may also be compact shell interaction. Our model predicts slow expansion of the radio sources and the appearance of new sources with diameters comparable to those of the present sources. This interpretation requires that the starburst nuclei have a large population of massive star supernova progenitors in a blue evolutionary phase. Our model can also be applied to the interaction of SN1987A with its circumstellar shell expected to occur within decades.

I. INTRODUCTION

Massive stars are known to strongly modify their environment through ionizing radiation and stellar winds. When the star explodes as a supernova, its primary interaction may be with circumstellar matter (i.e. matter modified by the progenitor star) out to a radius of 10's of pc (see McKee 1988 for a review). The radiation from a main sequence O star is able to evaporate clouds out to a radius $R_h \simeq 56\ n_m^{-0.3}$ pc where n_m is the mean density of the surrounding interstellar medium. The stellar wind creates a low density bubble in the region out to a radius R_b, where a swept up shell is present. In general, $R_b < R_h$, although for a strong wind R_b can reach R_h and radiative losses then slow the bubble evolution (McKee, van Buren, and Lazareff 1984). After the main sequence phase, the massive star evolves to become a red supergiant, which has a slow, dense wind. Most Type II supernovae are the explosions of stars at this point in their evolution and the interaction with the dense wind can give observable radio emission (Chevalier 1982b; Weiler et al. 1986). However, some stars evolve back to the blue before exploding. Possible examples of such objects are Wolf-Rayet stars and Sk -69 202, the progenitor of SN1987A. During the late blue phase, a fast stellar wind is again expected which can drive a shell in the red supergiant wind. Shells have been observed around some Wolf-Rayet stars (Chu, Treffers, and Kwitter 1983) and a shell is likely to exist around SN1987A (Fransson et al. 1989).

The interaction of supernovae with circumstellar bubbles has already received some attention. Fabian, Brinkmann, and Stewart (1983) computed the expansion of a supernova into an extended wind region and found approximate free expansion out to a large radius. Charles, Kahn, and McKee (1985) argued that the lack of clouds inside the Cygnus Loop implies that it is the remnant of a high mass star, and that the presence of filaments within 20 pc of the

center limits the spectral type of the progenitor to later than BO. The circular appearance of the Cygnus Loop, together with the recent interaction with moderately dense gas, suggests an interaction with a circumstellar shell. Shull et al. (1985) developed a model for the remnant N49 based on the hypothesis that photoionization by a B type progenitor star created a shell that subsequently expanded into the cavity during the star's red supergiant phase. Circumstellar interaction models have also been proposed for N 132D (Hughes 1987) and Kepler's remnant (Bandiera 1987).

Our purpose here is to examine the interaction of a massive star supernova with the shell created by a blue supergiant wind, either in the main sequence phase or in a late evolutionary phase. We make a number of idealizations so that the general features of shell interaction can be described by semi-analytic solutions. In §II, we discuss the expected properties of the supernova and its environment. The hydrodynamics of the interaction is described in §III. Special attention is given to self-similar flows. Applications to observed objects are given in §IV.

II. SUPERNOVAE AND THEIR ENVIRONMENTS

a) Supernovae

The result of a massive star supernova many days after the explosion is freely expanding gas with $v = r/t$, where v is the velocity, r is the radius, and t is the time from the explosion. The density profile in the outer part of the supernova can be described by a steep power law in radius $\rho \propto r^{-n}$ (Jones, Smith, and Straka 1981; Chevalier and Soker 1989). For example, numerical computations for the explosion of SN1987A give $n \simeq 9.6$ (Arnett 1988). The inner part of the density profile is moderately flat and we approximate it by constant density. We also assume that there is a sharp transition between these 2 regions at a velocity v_t, although in an actual case a gradual transition is likely. The density profile is then described by

$$\rho = \begin{cases} F\, t^{-3} & v < v_t \\ F\, t^{-3} (v/v_t)^{-n} & v \geq v_t \end{cases} \qquad (2.1)$$

where

$$F = \frac{1}{4\pi n} \frac{[3(n-3)M_{ej}]^{5/2}}{[10(n-5)E]^{3/2}} ,$$

$$v_t = \left[\frac{10}{3} \frac{(n-5)}{(n-3)} \frac{E}{M_{ej}}\right]^{1/2} ,$$

and E and M_{ej} are the total energy and mass in the explosion. The pressure in the expanding gas is negligible. We note that the density profile is modified if the supernova interacts with a red giant wind before expanding into the bubble (Band and Liang 1988; Itoh and Masai 1989), as might be expected for interaction with a main sequence star bubble. If the mass in the red giant wind is small compared to that of the supernova, the effect on our results is small.

b) Main Sequence Stars

Table 1 gives some of the typical wind properties of massive stars on the main sequence as compiled by Abbott (1982) and Garmany et al. (1981). The lifetime is that on the main sequence, $\dot{M}$ is the mass loss rate and v_w is the wind velocity. It can be seen that for the lower mass stars, the fraction of the stellar mass that is lost is relatively small, while for the most massive stars, a significant fraction of the star may be lost. The very massive stars are likely to become Wolf-Rayet stars (Chiosi and Maeder 1986). Weaver et al. (1977) give a detailed description of the bubble that is created by the interaction of the wind with a uniform medium. Here we use a simplified model which keeps the basic features of the bubble structure. Weaver et al. (1977) describe three phases of evolution: an early phase that is completely adiabatic and lasts several 10^3 years, an intermediate phase in which the swept-up interstellar medium cools and forms a shell, and a late phase when radiative losses from the shocked wind gas become important. At the times of interest here, the outer shell is expected to cool. However, we differ from Weaver et al. (1977) by assuming that heat conduction between the cool shell and the hot bubble is reduced by magnetic effects. The reason for this assumption is that the magnetic field in the stellar wind is expected to become tangential, as in the case of the solar heliosphere. Unless magnetic reconnection significantly changes the magnetic field geometry, the cool shell and the hot bubble are well shielded from each other. Under these circumstances, there is not much gas at intermediate temperatures and densities where radiative cooling becomes important, so that the bubble does not enter the final radiative phase within its lifetime.

For a fast stellar wind, the hot shocked gas fills the bubble volume and the gas pressure is uniform inside this volume. Assuming that the hot gas

drives a thin shell into gas of density ρ_o, the shell radius and the interior pressure are (Weaver et al. 1977):

$$R = \left(\frac{250}{308\pi}\right)^{1/5} L_w^{1/5} \rho_o^{-1/5} t_w^{3/5} = 0.76\, L_w^{1/5} \rho_o^{-1/5} t_w^{3/5} \qquad (2.2)$$

and

$$p = \frac{7}{(3850\pi)^{2/5}} L_w^{2/5} \rho_o^{3/5} t_w^{-4/5} = 0.16\, L_w^{2/5} \rho_o^{3/5} t_w^{-4/5} \qquad (2.3)$$

where $L_w = 1/2\ \dot{M}\ v_w^2$, and t_w is the time from the initiation of the wind. Table 1 gives the shell radius at the end of the main sequence lifetime. Some further expansion of the bubble can occur during the post-main sequence phases.

The shell velocity is $0.6\ R/t_w$ and drops below 10 km s^{-1} for the lower mass stars. These velocities are sufficiently low that the interstellar pressure may cause stagnation of the bubble at a radius somewhat smaller than that given in Table 1. This is particularly true if the external gas is photoionized by radiation from the central star. Weaver et al. (1977) note that the time when the ionization front is trapped in the outer shell is approximately equal to the time when the shell stagnates. Thus the ionization front may never be trapped. McKee, van Buren, and Lazareff (1984) have studied the case of HII region and bubble evolution in a cloudy interstellar medium and also found that massive stars can generally photoionize the bubble shells. If the gas is photoionized, the temperature is about 8000K and the sound speed is about 10 km s^{-1}. If the gas cools and recombines, the temperature may drop to 100K and the sound speed to 1 km s^{-1}. If the shell velocity is significantly greater than the ambient sound speed, c_o, the compression is

$$\frac{\rho_s}{\rho_o} = \frac{(v_s^2 + c_o^2)}{c_s^2} \qquad (2.4)$$

where ρ_s and c_s are the density and the sound speed in the shell. If the swept-up gas is photoionized, a star at the end of its main sequence life may not create a well-defined shell, but create a hole in an HII region.

Weaver et al. (1977) show that the density inside the hot bubble is quite uniform, except for a sharp rise close to the contact discontinuity, at radius R_d. The density increases by a factor of 2 over its interior value at a radius 0.98 R_d. Since there is a large density jump between the bubble and the exterior region, the assumption of uniform density throughout is adequate. The density inside the bubble is then

$$\rho_b = 2.0 \times 10^{-27} \left(\frac{M_l}{M_\odot}\right) \left(\frac{R}{20\ \mathrm{pc}}\right)^{-3} \mathrm{g\ cm^{-3}} \qquad (2.5)$$

where M_l is the mass lost in the fast main sequence wind. The temperature in the bubble is

$$T_b = 0.15 \frac{\bar{m}\, v_w^2}{k} = 1.1 \times 10^7 \left(\frac{v_w}{10^3\ \mathrm{km\ s^{-1}}}\right)^2 \mathrm{K} \qquad (2.6)$$

where $\bar{m}$ is the mean particle mass and k is Boltzmann's constant.

There are possible complications to this simple picture of bubble structure. One is that the star can have a space velocity that carries it close to one side of the shell; then a bow shock type structure occurs (Weaver et al. 1977). Another is that O stars tend to occur in clusters so that the interstellar medium may be affected by the winds from many stars. These factors may obscure shell-type structure.

c) Wolf-Rayet and Related Stars

The bubbles created by main sequence stars are large and diffuse so the lack of observational data on such objects is not surprising. However, a number of Wolf-Rayet stars are surrounded by shells (see Chu et al. 1983 for a summary on these objects). These shells typically have radii of 3-10 pc,

velocities of 30-100 km s^{-1} and densities of 300-1000 cm^{-3}. The nebula NGC 6888 has an estimated mass of 3.6 $M_\odot$, while other nebula have higher estimated masses. We believe that many of the ring nebulae are mass loss from a previous red supergiant phase that has been swept up by the Wolf-Rayet star wind (Wendker et al. 1975; Chevalier and Imamura 1983; McCray 1983). One factor in favor of this hypothesis is the He and N abundance enhancements observed in some ring nebulae (Kwitter 1981, 1984). Another is the fact that ionizing radiation and winds from main sequence massive stars clear out a region at least 20 pc in radius, so the presence of dense gas close to the star indicates that it is the product of mass loss (McKee 1988).

The detailed structure resulting from the interaction of two winds is discussed by Chevalier and Imamura (1983). For typical parameters, we expect the outer shock wave to be radiative while the inner shocked gas is adiabatic. There may be cases in which the inner shock radius R_1 is not $<< R$. From the results of Chevalier and Imamura (1983), $R_1 \geq 0.5\ R$ for $v_w \leq 10\ v_s$. Most Wolf-Rayet stars do have fast winds with $v_w \sim 2000$ km s^{-1} so that the shocked wind gas should fill most of the volume. If the shell velocity is significantly greater than that of the red supergiant wind, then the shell velocity is

$$v_s \approx \left(\frac{\dot{M}_b\, v_b^2 v_r}{3\dot{M}_r}\right)^{1/3} \tag{2.7}$$

where $\dot{M}$, v_b, and v_r are the mass loss rate and the wind velocity in the blue (b) and the red (r) phases, respectively. Data on observed Wolf-Rayet bubbles indicate that they are expanding less rapidly than would be expected if the energy of the inner wind were conserved (Treffers and Chu 1982; Chevalier and Imamura 1983; McCray 1983). One possibility is that the shell is subject to Rayleigh-Taylor instabilities so that it fragments and hot gas is able to

pass through the shell. X-ray observations of NGC 6888 have given some direct evidence for this process (Bochkarev 1988).

Although the progenitor of SN1987A was not a Wolf-Rayet star, it was an early-type supergiant that was surrounded by a circumstellar shell. The observed N overabundance and low velocity of the circumstellar material (Fransson et al. 1989) suggests that it is material lost in a red supergiant wind that was swept up by the blue supergiant wind. The blue progenitor is estimated to have $\dot{M}_b$ of a few 10^{-6} $M_\odot$ yr^{-1} and v_b = 550 km s^{-1}. Chevalier (1987, 1988) describes the hydrodynamics of this situation. The evolution and relative intensities of the ultraviolet emission lines suggest a radius of about 5 x 10^{17} cm (Sonneborn et al. 1988) and a density $n_c \simeq$ (1-3) x 10^4 cm^{-3} (Fransson et al. 1989). The age of the shell is probably 10^4 yr, so that the amount of shocked fast wind gas is about 0.03 $M_\odot$.

III. HYDRODYNAMICS OF THE INTERACTION

a) Initial Shell Interaction

The results from §II indicate that the mass of hot shocked gas inside the bubble is likely to be smaller than the mass in the outer power law region of the expanding supernova. Thus the interaction is with a density profile of the form $\rho = A\ r^{-n}\ t^{n-3}$ where $A = Fv_t^n$. In the bubble region, most of the volume is occupied by a gas at a constant density $\rho = B$, where $B = 3M_1/(4\pi R^3)$. The interaction within the bubble gives a double shock structure that is described by a self-similar solution (Chevalier 1982a). The outer shock wave has a radius

$$R_2 = (\alpha \frac{A}{B})^{1/n}\ t^{\frac{n-3}{n}} \tag{3.1}$$

where α is a number that can be deduced from the discussion in Chevalier (1982a). For example, for n=6, α=4.9 and for n=9, α=1.5. The application of this solution through the bubble region requires that the mass of ejecta in the power-law region be greater than the amount of shocked ejecta when the interaction region reaches the edge of the bubble, or $3M_{ej}/n > \zeta\ M_1$, where $\zeta = 0.28$ for $n = 6$ and $\zeta = 0.93$ for $n = 9$.

The properties at the time of the initial interactions with the shell can be determined from the solution. The time to the interaction is

$$t_i = [\frac{n\ M_1}{(n-3)\alpha M_{ej}}]^{\frac{1}{n-3}}\ \frac{R}{v_t}, \tag{3.2}$$

the shock velocity just before the interaction is

$$v_i = \frac{(n-3)}{n}\ \frac{R}{t_i}\ , \tag{3.3}$$

and the postshock pressure is

$$p_i = \frac{9}{16\pi}\left(\frac{n-3}{n}\right)^{\frac{2(n-2)}{(n-3)}} \alpha^{\frac{2}{n-3}} \frac{M_l}{R^3}\left(\frac{M_{ej}}{M_l}\right)^{\frac{2}{n-3}} v_t^2 \qquad (3.4)$$

For n = 9, we note that the characteristic supernova interaction time is

$$t_s = \frac{R}{v_t} = 294\ \left(\frac{R}{pc}\right)\left(\frac{E}{10^{51}\ erg}\right)^{-1/2}\left(\frac{M_{ej}}{10M_\odot}\right)^{-1/2}\ yr \qquad (3.5)$$

and that

$$t_i = 0.605\left(\frac{M_l/M_{ej}}{0.05}\right)^{1/6} t_s .$$

For the cases of interest here, there is a large density contrast between the bubble and the shell so that the amount of energy transmitted into the shell is initially small. When the interaction region hits the wall, the kinetic energy of the flow is converted to thermal energy and the postshock pressure is increased by a factor β up to 6 (Silk and Solinger 1973). The increased pressure drives a reflected shock wave back through the interaction region. The timescale for the reflected shock wave to traverse the interaction region is roughly $\Delta R_i/(2v_i)$ where ΔR_i is the initial thickness of the interaction region (see Chevalier 1982a) and the factor of 2 is to approximately take into account the backward motion of the reflected shock and the density structure within the interaction region.

This initial phase of shell interaction is well illustrated by the numerical computations of Dickel and Jones (1985). Their model for Tycho's remnant has a supernova with $E = 9.9 \times 10^{50}$ ergs, $M_{ej} = 2.45\ M_\odot$, and n=7, and a "bubble" with $M_l = 0.67\ M_\odot$ and $R = 6.9 \times 10^{18}$ cm. The motion of the reflected shock front through the interaction region is clearly shown in their calculation. They chose a shell with a relatively small density contrast with the uniform medium (a factor of 2.2), so that there was considerable transmission of energy into and through the shell.

b) The Shocked Supernova Gas

For many cases of interest here, $M_1 << M_{ej}$ so that the outer steep power law part of the supernova density profile continues to interact with the shell. The density distribution is given by $\rho = Ar^{-n} t^{n-3}$. As noted above, the energy initially transmitted into the shell at radius R is small. Under these circumstances, the flow is described by two parameters, A and R, and we expect it to have a self-similar nature. One of the parameters has the dimensions of a radius so we expect that the shock radius, R_s, is constant in time. The physical reason for this is that the rising ram pressure of the ejecta continuously compresses the shocked ejecta so that the total volume of the shocked ejecta remains constant. In this subsection, we focus our attention on the shocked ejecta on the assumption that the shell radius R remains constant. In the next subsection, we treat the transmitted shock in the shell.

The self-similar variables are taken to be

$$\eta = \frac{r}{R_s}, \quad v = R_s t^{-1} U(\eta), \quad \rho = Ct^{n-3}\Omega(\eta), \quad p = CR_s^2 t^{n-5} P(\eta) \tag{3.6}$$

where C is a constant and η, U, Ω, and P are dimensionless variables for the radius, velocity, density and pressure. When these variables are substituted into the spherically symmetric fluid equations for conservation of mass, momentum, and energy, the resulting equations are

$$(n-3) + \frac{U\Omega'}{\Omega} + U' + \frac{2U}{\eta} = 0 \tag{3.7}$$

$$U(U'-1) + \frac{P'}{\Omega} = 0 \tag{3.8}$$

$$n - 5 - \gamma (n-3) + U[\frac{P'}{P} - \gamma \frac{\Omega'}{\Omega}] = 0 \tag{3.9}$$

where γ is the adiabatic index and the prime represents $d/d\eta$. The equations can be combined to yield

$$U' = \frac{\frac{n-5}{\gamma} + \frac{2U}{\eta} + \frac{\Omega U^2}{\gamma P}}{\frac{\Omega U^2}{\gamma P} - 1} \tag{3.10}$$

and two other equations for the first derivatives. Taking $C = AR_s^{-n}$, the boundary conditions at the shock front are

$$U(1) = \frac{\gamma-1}{\gamma+1}, \quad \Omega(1) = \frac{\gamma+1}{\gamma-1}, \quad P(1) = \frac{2}{\gamma+1}. \tag{3.11}$$

The integration of this set of equations from η=1 out to where U=0 is straightforward and the solution for γ=5/3 and n=9 is illustrated in fig. 1. Table 2 lists R_s/R and $p(R)/p_s$, where R is the shell radius and p_s is the immediate postshock pressure for various values of n.

Approximate solutions for the flow can be obtained by assuming that the flow is highly subsonic, i.e. $\Omega U^2/\gamma P << 1$. This assumption is very accurate close to R and becomes less accurate close to R_s. Dropping the $\Omega U^2/\gamma P$ terms in eqn. (3.10) leads to

$$U = \frac{(n-5)}{3\gamma\eta^2}(\eta_R^3 - \eta^3) \tag{3.12}$$

where η_R is the value of η at R; we note that $1/\eta_R = R_s/R$. By imposing the shock boundary condition on U(1), we find

$$\eta_R = \left[1 + \frac{3\gamma(\gamma-1)}{(\gamma+1)(n-5)}\right]^{1/3}. \tag{3.13}$$

For γ=5/3 and n=6 and 9, this expression gives values of $(R-R_s)/R_s$ that are large by 7%. The tendency of R_s to approach r=0 as n approaches 5 is clear.

Combining eqns. (3.7) and (3.12) and the shock boundary condition on Ω yields

$$\Omega = \left(\frac{\gamma+1}{\gamma-1}\right)\left(\frac{\eta_R^3 - \eta^3}{\eta_R^2 - 1}\right)^{\frac{\gamma(n-3)}{n-5}-1} \tag{3.14}$$

as the result of mass conservation. This expression shows the tendency for

the density to be peaked at the shock front as n approaches 5. The subsonic flow assumption implies a uniform pressure region; however, a drop in pressure is expected close to the shock front. We find an approximate value for the interior pressure p_{int} by equating the total energy in the shocked region

$$T = \int_{R_s}^{\infty} \frac{1}{2} A r^{-n} t^{n-3} v^2 4\pi r^2 dr = \frac{2\pi}{(n-5)} A R_s^{5-n} t^{n-5}$$

with the internal energy in the shocked gas. The solutions show that the kinetic energy in the shocked gas is small ($\lesssim$ 2% of T). The ratio of p_{int} to the postshock pressure is

$$\frac{p_{int}}{p(R_s)} = \frac{3(\gamma+1)\ (\gamma-1)}{4(n-5)\ (\eta_R^3 - 1)} \quad . \tag{3.15}$$

The pressure at the shell interface is the same as p_{int}, so we have

$$p(R) = \frac{(\gamma-1)}{2\gamma} \left[1 + \frac{3\gamma(\gamma-1)}{(\gamma+1)\ (n-5)}\right]^{\frac{n-2}{3}} R^{2-n} A t^{n-5} \quad . \tag{3.16}$$

The value of p(R) is important for determining the effect of the shocked supernova gas on the shell gas. While we have derived expressions for a general γ, all of our applications assume γ=5/3.

The self-similar solution discussed here is asymptotically approached for t >> t_i. The timescale after t_i on which the solution begins to have relevance is the thickness of the shocked region divided by a typical velocity, or t(R-R_s)/R. Table 2 shows that this is about 0.1t for n = 9. The part of the shocked flow close to the shell will retain characteristics of the shocked interaction region in the circumstellar bubble.

c) The Shocked Shell Gas

The pressure generated by the shocked supernova gas is expected to drive a shock wave into the cool circumstellar shell gas which has a density ρ_c. If the shock front is radiative, the shell gas is swept up into a thin shell of mass M_c and velocity v_c. We assume that the distance traveled by the shock is

<<R so that the flow is approximately planar. The motion of the shell is determined by

$$\frac{dM_c}{dt} = 4\pi R^2 \rho_c \frac{dR_c}{dt} \tag{3.17}$$

and

$$M_c \frac{dv_c}{dt} = 4\pi R^2 [p(R) - \rho_c v_c^2] \tag{3.18}$$

where R_c is the radius of the shock front in the shell. During the initial interaction, the pressure is a factor β times the value given in eqn. (3.4) and we have

$$R_c = R + \left(\frac{\beta p_i}{\rho_c}\right)^{1/2} (t - t_i), \tag{3.19}$$

where β is approximately 6. Later, the pressure increases as in eqn. (3.16), which can be written $p(R) = KAR^{2-n}t^{n-5}$, where K is a dimensionless constant. For n=6, K=0.87 and for n=9, K=0.86. In this case, the shock wave accelerates as

$$R_c = R + \left[\frac{2\ KAR^{2-n}}{(n-3)\ (n-4)\ \rho_c}\right]^{1/2} t^{\frac{n-3}{2}} . \tag{3.20}$$

We have assumed that the shock front is radiative. If the flow is non-radiative, it can be described by a self-similar solution. Parker (1961) and Chevalier (1984) have described similar solutions for spherically symmetric piston-driven flows. Fig. 2 shows the planar solution for n=9. As expected for an accelerating flow (Chevalier 1984), the density diverges at the contact discontinuity and the pressure increases inward from the shock front. The expansion law for the shock radius can be found from pressure continuity across the contrast discontinuity. If the shock radius is expressed as $R_c = R + K_1 (AR^{2-n} t^{n-3}/\rho_c)^{1/2}$, then for n=9, $K_1 = 0.26$ for the non-radiative

solution and $K_1 = 0.24$ in the thin shell case (from eqn. 3.20). The results from the thin shell solution adequately describe the dynamics even if the shell is non-radiative.

d) Late Evolution

We have described a phase of evolution during which the pressure in the shocked region is rising due to the interaction with the outer density profile of the supernova. The flow will eventually deviate from this evolution for three possible reasons: (1) the bend in the supernova density profile reaches the inner shock front; (2) the energy transferred to the shell gas becomes large compared to the energy in the shocked supernova gas; and (3) the shock wave in the circumstellar shell traverses the shell. We discuss the implications of each of these possibilities.

The timescale for the bend in the supernova profile to reach the shock front is

$$t_1 = \frac{t_s}{\eta_R} \tag{3.21}$$

where t_s is given by eqn. (3.5) and η_R by eqn. (3.13) or Table 2. For n=9, $t_1 = 0.92 t_s$. After t_1, the reverse shock wave moves to the center of the explosion, the pressure drops and a rarefaction wave moves through the high pressure interaction region. The propagation of the reverse shock to the center requires a detailed numerical calculation, but a rough estimate suggests that the time to reach the center is somewhat less than $2t_1$. Once the supernova energy is thermalized within the radius R, the final pressure is $E/(2\pi R^3)$. For n=9, the ratio of the final pressure to the peak pressure at time t_1 is 0.41.

Another timescale characterizes the interaction with the circumstellar shell; it is

$$t_c = \left(\frac{\rho_c R^n}{A}\right)^{\frac{1}{n-3}} = 290 \left(\frac{\rho_c}{10^{-22}\ \mathrm{g\ cm^{-3}}}\right)^{1/6} \left(\frac{R}{\mathrm{pc}}\right)^{3/2} \left(\frac{E}{10^{51}\ \mathrm{erg}}\right)^{-1/2} \left(\frac{M_{ej}}{10 M_\odot}\right)^{1/3} \mathrm{yr} \tag{3.22}$$

where the numerical value is for n=9. This timescale enters into the time at which the energy transferred into the shell becomes significant. The work done on the shell by the shocked supernova gas, W, is determined by

$$\frac{dW}{dt} = 4\pi R^2\ p(R)\ \frac{dR_c}{dt} \tag{3.23}$$

Using eqns. (3.16) and (3.20), we find the time at which W is equal to T/2 to be

$$t_2 = \left\{\frac{125}{2048} \frac{(n-4)(3n-13)^2}{(n-3)\ (n-5)^2} \left[1 + \frac{5}{4(n-5)}\right]^{-\frac{(n+1)}{3}}\right\}^{\frac{1}{n-3}} t_c\ . \tag{3.24}$$

For n=9, $t_2 = 0.80\ t_c$. Relative values of t_1 and t_2 are discussed in the next section. Once the energy transfer to the shell is significant, the flow is determined by the parameters A and ρ_c, and the flow gradually evolves toward the self-similar solution described by Chevalier (1982a). This is the same solution that describes the flow in the wind bubble. However, in the present case, effects 1 and 3 mentioned above will probably prevent the flow from closely approximating the self-similar solution. The solution does show that the pressure in the interaction region is expected to decrease after time t_2.

Another reason for a pressure decrease is that the shock wave in the shell reaches the edge of the shell. If the shock wave is driven by the power law part of the supernova density profile, this occurs at a time

$$t_{3a} = \left(\frac{\Delta R}{K_1 R}\right)^{\frac{2}{n-3}} t_c = 0.75 \left(\frac{\Delta R/R}{0.1}\right)^{1/3} t_c \tag{3.25}$$

where ΔR is the shell thickness and the numerical value is for n=9. Eqn. (3.25) assumes that the time t_{3a} is considerably larger than t_1. If this is

not the case, then a shock wave can pass through the shell during the initial interaction with the shocked layer from the bubble interaction. Under these circumstances, the time at which the shock front reaches the far edge of the shell is

$$t_{3b} = t_i + \frac{\Delta R}{v_{ci}} = t_i + \left(\frac{\rho_c}{\beta p_i}\right)^{1/2} \Delta R \quad , \tag{3.26}$$

where v_{ci} is the initial shock velocity in the shell. If $t_{3b} > t_{3a}$, then t_{3b} gives a better estimate of the time of shock breakout from the shell. Once the shell edge is reached, a rarefaction wave moves into the interaction region from the outside. The numerical computation by Dickel and Jones (1985) illustrates this phase of the evolution. If the density outside the shell is low, as might occur for a Wolf-Rayet star bubble, much of the shocked gas might re-enter a phase of free expansion. McKee (1988) has noted that a low circumstellar density out to 20 pc or more tends to muffle the effects of a massive star supernova.

IV. APPLICATIONS

The previous section described the interaction of a supernova with an idealized, spherically symmetric, circumstellar bubble. The supernova shock wave propagates in the low density bubble until a time t_i, when the shock front reaches the bubble shell. The pressure in the shocked region then rises as the steep part of the supernova density profile interacts with the shell. The pressure rise stops when either the bend in the supernova density profile reaches the shock front (time t_1), the energy transfer to the shell is significant (time t_2), or the outer shock front propagates through the shell (time t_3). Table 3 gives some estimated timescales for interactions involving a main sequence star bubble, a Wolf-Rayet star bubble, and the shell around SN1987A. The values of R, ρ_c, and M_c are estimated from observational data (see §II) and ΔR is derived from $M_c = 4\pi R^2 \Delta R \rho_c$. The assumed supernova parameters are $E = 10^{51}$ ergs, $M_{ej} = 10 M_\odot$, and n=9. The upper part of Table 3 gives the assumed bubble parameters and the lower part gives the resulting timescales. We note that the derivation of the timescales t_2 and t_{3a} assumes that they are much larger than t_i. For the cases where $t_{3a} \lesssim t_i$, the timescale t_{3b} gives an estimate of the time at which the shock wave has propagated through the shell. Table 3 indicates that generally the shock waves are able to propagate through the shells before the energy transfer to the shell becomes significant.

From an observational point of view, it is important whether the shock front driven into the shell is radiative. From eqn. (3.19), the initial velocity of the shock front, v_{ci}, for the cases listed in Table 3 is given in the last row. The shock wave accelerates after the initial interaction because of the interaction with the outer supernova density profile and because of the breakout from the shell. Whether the shock becomes radiative

while traversing the shell can be estimated by comparing the column density through the shell with the column density needed for a radiative shock (McKee and Hollenbach 1980). For the cases listed in Table 3, radiative shocks are expected for the main sequence star case, the SN1987A shell is initially nonradiative, and the column density through the Wolf-Rayet star shell is approximately equal to that needed for cooling. Nonradiative shock waves can develop later in the evolution due to the acceleration effect.

The model presented here cannot be expected to give a detailed description of supernova remnants where bubble interaction is occurring, because instabilities and asymmetric structure undoubtedly play a role in the morphology, but it should describe the large-scale structure. Here we concentrate on Cas A, which is very likely to be a supernova interaction with a Wolf-Rayet star bubble. The presence of the quasi-stationary flocculi (QSF) with enhanced N and He abundances (Chevalier and Kirshner 1978) at a distance of 1.5 pc from the center of expansion is very suggestive of a Wolf-Rayet star wind bubble (see also Fesen, Becker, and Blair 1987). One difference with our model is the presence of fast moving knots (FMK) of heavy element gas, which shows that the supernova ejecta were clumpy and not smooth as we have assumed here. However, we assume that the observed knots are embedded in relatively smooth ejecta which dominate the interaction.

The X-ray structure of Cas A can be described by a bright inner shell with inner radius 102" and 17" thickness and a faint outer plateau region bounded by a weak shell with inner radius of 140" and about 20" thick (Fabian et al. 1980). At a distance of 2.8 kpc, 100" is 1.36 pc. The bright shell is also present at radio and optical wavelengths and there is a general correspondence between the structure in the three wavelength bands (Fabian et al. 1980; Dickel et al. 1982). We propose that the bright inner ring is the shocked

bubble shell. Where the shell density was high ($\gtrsim$ several 10^2 cm^{-3}), the shock waves became radiative and QSFs were the result; the lower density shell was shocked to X-ray emitting temperatures. The shock front has crossed the shell over much of surface area, and some combination of expansion of the shell gas and penetration of hot inner gas drives the outer plateau region. The cellular structure of the bright radio shell is likely to be due to Rayleigh-Taylor instabilities in the shell (Gull 1973; Bell, Gull, and Kenderdine 1975). Our model naturally produces the low expansion velocities observed for radio features (Bell 1977; Dickel and Greisen 1979; Tuffs 1986). We expect that the expansion would have been small at the time of initial shell interaction and may still be accelerating at the present time. The FMKs are freely expanding dense knots which light up when they enter the high pressure region. Based on no significant change in the large-scale optical structure over a period of 18 years, van den Bergh and Dodd (1970) conjectured that the FMKs were supernova fragments plowing through stationary interstellar cloud banks. While new radio features also appear due to this continued interaction (Dickel and Greisen 1979), the total radio flux is generally declining (Dent, Aller, and Olsen 1974) because the shell pressure is now dropping after the shock wave has passed through.

The main prediction of our model is that the bright observed ring is not the reverse shock wave of the supernova as is often assumed, but is the shocked bubble shell. The reverse shock wave is inside of the bright shell, as is hot ($T \sim 10^7 - 10^8$ K) shocked supernova ejecta. The cooler X-ray emission is from shocked circumstellar gas, although some FMK gas may be mixed in. The X-ray ring spectrum of Cas A is roughly consistent with normal abundances (Fabian et al. 1980).

Cas A is the most luminous radio supernova remnant in the Galaxy. We

believe that this is due to the presence of a dense circumstellar shell near the explosion. Other remnants where this might occur are the class of oxygen-rich supernova remnants. One of these, the source in NGC 4449, is a remarkably bright radio and X-ray source (Blair, Kirshner, and Winkler 1983) and is an excellent candidate for shell interaction. The remnant has a radio luminosity 25 times that of Cas A, an X-ray luminosity 100 times that of Cas A, and a thermal energy density about 10 times larger; Blair, Kirshner, and Winkler (1983) suggest that the remnant has a radius of 0.4 pc, an age of ~100 yr, and is expanding into a medium with a uniform density of 25 cm^{-3}. The present model would predict a relatively slow expansion of the radio source if it can eventually be measured by long baseline techniques.

Another class of objects which may involve shell interaction are compact radio sources in starburst galaxy nuclei. A particularly good example of this is the set of 23 sources in M82 (Kronberg, Biermann, and Schwab 1985; Bartel et al. 1987b). These sources have radio diameters $\gtrsim$ 0.3 - 1 pc and $\lesssim$ 2.7 - 5.4 pc; their radio luminosities are between several times and 40 times that of Cas A, except for 41.9 + 58, which has a luminosity about 150 times that of Cas A. Bartel et al. (1987a) suggest that the steep spectrum observed for some of the sources argues against a supernova remnant interpretation. However, when a source first turns on as a radio source, a steep spectrum might be expected. The spectrum of Cas A is moderately steep and is observed to be flattening with time (Dent, Aller, and Olsen 1974). A similar set of 35 compact radio sources has been observed in NGC 253 (Antonucci and Ulvestad 1988). These sources are unresolved or partially resolved at a diameter of 2-5 pc and have radio luminosities comparable to that of Cas A.

A prediction of the present model is that the radio sources should have relatively small expansion velocities. Assuming a radial expansion velocity

of 6000 km s^{-1}, Bartel et al. (1987b) and Antonucci and Ulvestad (1988) deduced the formation rate of the sources in both M82 and NGC 253 to be 0.1 yr^{-1}. If our model is correct, these results could overestimate the formation rate by a factor of about 2. However, Kronberg and Sramek (1985) deduced a formation rate in M82 of 0.2-0.3 yr^{-1} based on the flux decay rate of the observed sources. This method of estimating the formation rate should apply in our model. If their rate is accurate, a new compact source may be observed in M82 in the near future. Our model predicts that the radio size of a new source should be comparable to the sizes of the presently observed sources. This would not be the case if the sources were "radio supernovae" (Weiler et al. 1986).

The sizes of the inferred shells in the compact radio sources are somewhat smaller than those observed around galactic Wolf-Rayet stars, but the smaller ones have sizes comparable to the inferred shell around SN1987A. The high rate of formation of these objects in starburst galaxy nuclei suggests that massive stars in these nuclei frequently become red supergiants and then evolve to the blue before exploding as supernovae. The evolution to the blue could be due to either extreme mass loss or to the conditions, which are unclear at present, that gave rise to the late blueward evolution of the SN1987A progenitor star.

The remnant of SN1987A will provide a particularly informative example of bubble interaction because we already have detailed observational data on the supernova properties and on the circumstellar shell. From Table 3, the interaction will start at an age of 18 years, but this is uncertain because of uncertainties in the shell radius and in the bubble density. Masai et al. (1987) proposed that the soft X-ray emission observed from SN1987A beginning half a year after the explosion is due to circumstellar interaction, but this

hypothesis may have difficulty with the observed variability of the source (Chevalier 1988). In our model, when the shock wave reaches the shell at an age of 18 years it heats the shell gas to a temperature of 4×10^6K. The cooling time for this gas is more than 20 years, so the X-ray luminosity increases as the shock traverses the shell. In our spherical model, the time to cross the shell is somewhat less than a year, but in an actual case, irregular shell structure will increase the rise time. From the cooling rates of Gaetz and Salpeter (1983), the luminosity of the heated shell is 4×10^{38} $(M_c/0.1\ M_\odot)$ erg s^{-1}. It is not possible to theoretically calculate the expected nonthermal radio flux during the shell interaction phase, but a rough scaling from Cas A leads to a flux of 10 Jy at 1 GHz. The source size will be 1"-2". Since there is already evidence for asymmetries in the explosion of SN1987A (Cropper et al. 1988), asymmetries are expected in the shell interaction. SN1987A will provide a valuable example of shell interaction, but it will be more than a decade before the interaction unfolds.

We are grateful to the referee for helpful comments. This research was supported in part by NSF grant AST-8615555, NASA grant NAGW-764, and by the U. S. Department of Energy under contract number W-7405-ENG-48 to the Lawrence Livermore National Laboratory.

Table 1

Main Sequence Bubbles

Mass ($M_\odot$)	Spectral Type	Lifetime (10^6 yr)	$\dot{M}$ ($M_\odot$ yr^{-1})	v_w (km s^{-1})	$Rn_H^{0.2}$ (pc cm$^{-3/5}$)
100	O4V	3.4	5×10^{-6}	3000	92
60	O6V	4.2	1×10^{-6}	3000	76
20	O9V	10.3	6×10^{-8}	2500	69
15	B0.5V	11.1	6×10^{-9}	2500	45

Table 2

Properties of the Shocked Supernova Gas

n	R_s/R	$p(R)/p_s$
5.5	0.678	1.166
6	0.774	1.160
7	0.858	1.153
8	0.896	1.149
9	0.917	1.146
10	0.932	1.144
12	0.949	1.141
14	0.960	1.140
16	0.966	1.139

Table 3

Properties of Bubble Interaction

	Main Sequence Star	Wolf-Rayet Star	SN1987A
R(cm)	10^{20}	10^{19}	5×10^{17}
ρ_c(g cm^{-3})	10^{-23}	2×10^{-22}	4×10^{-20}
M_c ($M_\odot$)	400	5	0.1
ΔR (cm)	6.4×10^{17}	4.0×10^{16}	1.6×10^{15}
M_1 ($M_\odot$)	2	0.3	0.03
t_i (yr)	7,300	530	18
t_1 (yr)	8,800	880	44
t_2 (yr)	29,000	1,500	41
t_{3a} (yr)	11,000	490	12
t_{3b} (yr)	10,500	580	19
v_{ci} (km s^{-1})	60	230	660

REFERENCES

Abbott, D. C. 1982, Ap. J., 263, 723.

Antonucci, R. R. J. and Ulvestad, J. S. 1988, Ap. J. (Letters), 330, L97.

Arnett, W. D. 1988, Ap. J., 331, 377.

Band, D. L. and Liang, E. P. 1988, Ap. J., 334, 266.

Bandiera, R. 1987, Ap. J., 319, 885.

Bartel, N., Ratner, M. I., Rogers, A. E. E., Shapiro, I. I., Bonometti, R. J., Cohen, N. L., Gorenstein, M. V., Marcaide, J. M., and Preston, R. A. 1987b, Ap. J., 323, 505.

Bartel, N., Ratner, M., Shapiro, I., and Rogers, A. 1987a, in IAU Symposium 121, Observational Evidence of Activity in Galaxies, ed. E. Ye. Kachikian, K. J. Fricke, and J. Melnick (Dordrecht: Reidel), p. 521.

Bell, A. R. 1977, M.N.R.A.S., 179, 573.

Bell, A. R., Gull, S. F., and Kenderdine, S. K. 1975, Nature, 257, 463.

Blair, W. P., Kirshner, R. P., and Winkler, P. F., Jr. 1983, Ap. J., 272, 84.

Bochkarev, N. G. 1988, Nature, 332, 518.

Charles, P. A., Kahn, S. M., and McKee, C. F. 1985, Ap. J., 295, 456.

Chevalier, R. A. 1982a, Ap. J., 258, 790.

Chevalier, R. A. 1982b, Ap. J., 259, 302.

Chevalier, R. A. 1984, Ap. J., 280, 797.

Chevalier, R. A. 1987, in ESO Workshop on SN1987A, ed. I. J. Danziger (Garching: ESO), p. 483.

Chevalier, R. A. 1988, Nature, 332, 514.

Chevalier, R. A. and Imamura, J. N. 1983, Ap. J., 270, 554.

Chevalier, R. A. and Kirshner, R. P. 1978, Ap. J., 219, 931.

Chevalier, R. A. and Soker, N. 1989, Ap. J., in press (June 15).

Chiosi, C. and Maeder, A. 1986, Ann. Rev. Astr. Ap., 24, 329.

Chu, Y.-H., Treffers, R. R., and Kwitter, K. B. 1983, Ap. J. Suppl., 53, 937.

Cropper, M., Bailey, J., McCowage, J., Cannon, R. D., Couch, W. G., Walsh, J. R., Strade, J. O. and Freeman, F. 1988, M.N.R.A.S., 231, 695.

Dent, W. A., Aller, H. D., and Olsen, E. T. 1974, Ap. J. (Letters), 188, L11.

Dickel, J. R. and Greisen, E. W. 1979, Astr. Ap., 75, 44.

Dickel, J. R. and Jones, E. M. 1985, Ap. J., 288, 707.

Dickel, J. R., Murray, S. S., Morris, J., and Wells, D. C. 1982, Ap. J., 257, 145.

Fabian, A. C., Brinkmann, W., and Stewart, G. C. 1983, in IAU Symp. 101, Supernova Remnants and Their X-Ray Emission, eds. J. Danziger and P. Gorenstein (Dordrecht: Reidel), p. 119.

Fabian, A. C., Willingale, R., Pye, J. P., Murray, S. S., and Fabbiano, G. 1980, M.N.R.A.S., 193, 175.

Fesen, R. A., Becker, R. H., and Blair, W. P. 1987, Ap. J., 313, 378.

Fransson, C., Cassatella, A., Gilmozzi, R., Kirshner, R. P., Panagia, N., Sonneborn, G., and Wamsteker, W. 1989, Ap. J., 336, 429.

Gaetz, T. J. and Salpeter, E. E. 1983, Ap. J. Suppl., 52, 155.

Garmany, C. D., Olson, G. L., Conti, P. S., and van Steenberg, M. E. 1981, Ap. J., 250, 660.

Gull, S. F. 1973, M.N.R.A.S., 162, 135.

Hughes, J. P. 1987, Ap. J., 314, 103.

Itoh, H. and Masai, K. 1989, M.N.R.A.S., in press.

Jones, E. M., Smith, B. W., and Straka, W. C. 1981, Ap. J.,

Kronberg, P. P., Biermann, P., and Schwab, F. R. 1985, Ap. J., 291, 693.

Kronberg, P. P. and Sramek, R. A. 1985, Science, 227, 28.

Kwitter, K. B. 1981, Ap. J., 245, 154.

Kwitter, K. B. 1984, Ap. J., 287, 840.

Masai, K., Hayakawa, S., Itoh, H., and Nomoto, K. 1987, Nature, 330, 235.

McCray, R. A. 1983, Highlights of Astr., 6, 565.

McKee, C. F. 1988, in IAU Coll. 101, The Interaction of Supernova Remnants with the Interstellar Medium, eds. T. Landecker and R. Rogers (Cambridge: C. Univ. P.), p. 205.

McKee, C. F. and Hollenbach, D. J. 1980, Ann. Rev. Astr. Ap., 18, 219.

McKee, C. F., van Buren, D., and Lazareff, B. 1984, Ap. J. (Letters), 278, L115.

Parker, E. N. 1961, Ap. J., 133, 1014.

Shull, P., Jr., Dyson, J. E., Kahn, F. D., and West, K. A. 1985, M.N.R.A.S., 212, 799.

Silk, J. and Solinger, A. 1973, Nature Phys. Sci., 244, 101.

Sonneborn, G., Kirshner, R., Fransson, C., Cassatella, A., Wamsteker, W., Gilmozzi, R., and Panagia, N. 1988, I.A.U. Circ. No. 4685.

Treffers, R. R. and Chu, Y.-H. 1982, Ap. J., 254, 569.

Tuffs, R. J. 1986, M.N.R.A.S., 219, 13.

van den Bergh, S. and Dodd, W. W. 1970, Ap. J., 162, 485.

Weaver, R., McCray, R., Castor, J., Shapiro, P. R., and Moore, R. T. 1977, Ap. J., 218, 377.

Weiler, K. W., Sramek, R. A., Panagia, N., van der Hulst, J. M., and Salvati, M. 1986, Ap. J., 301, 790.

Wendker, H. J., Smith, L. F., Israel, F. P., Habing, H. J., and Dickel, H. R. 1975, Astr. Ap., 42, 173.

FIGURE CAPTIONS

Fig. 1 Plot of density (ρ), velocity (u), and pressure (p) of shocked ejecta material as functions of radius in units of reverse shock radius R_s for the self-similar solution with n=9, γ=5/3. All variables are normalized to their values at the shock front (subscripted s). Note that the density and velocity vanish at the contact surface (right boundary).

Fig. 2 Plot of density (ρ), velocity (u), and pressure (p) of shocked shell material as functions of radius for the planar self-similar solution with n=9, γ=5/3. R_c is the forward shock radius and R is the initial position of the inner edge of the dense shell. Here the density is normalized to ρ_c, the pressure to $\rho_c v_c^2$ and the velocity to v_c, where ρ_c is the ambient shell density and v_c is the shock velocity. Note that the density diverges at the contact surface (left boundary).

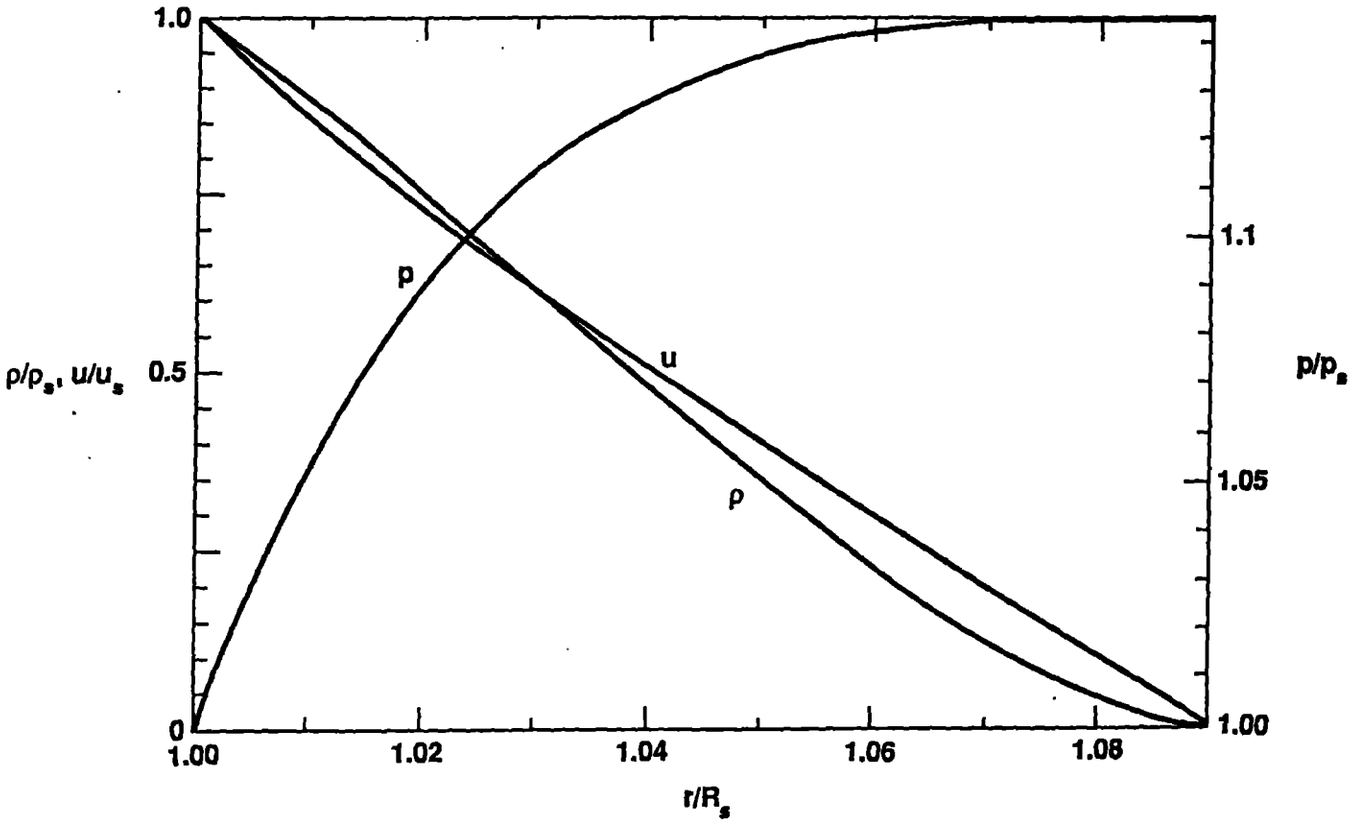

Fig. 1

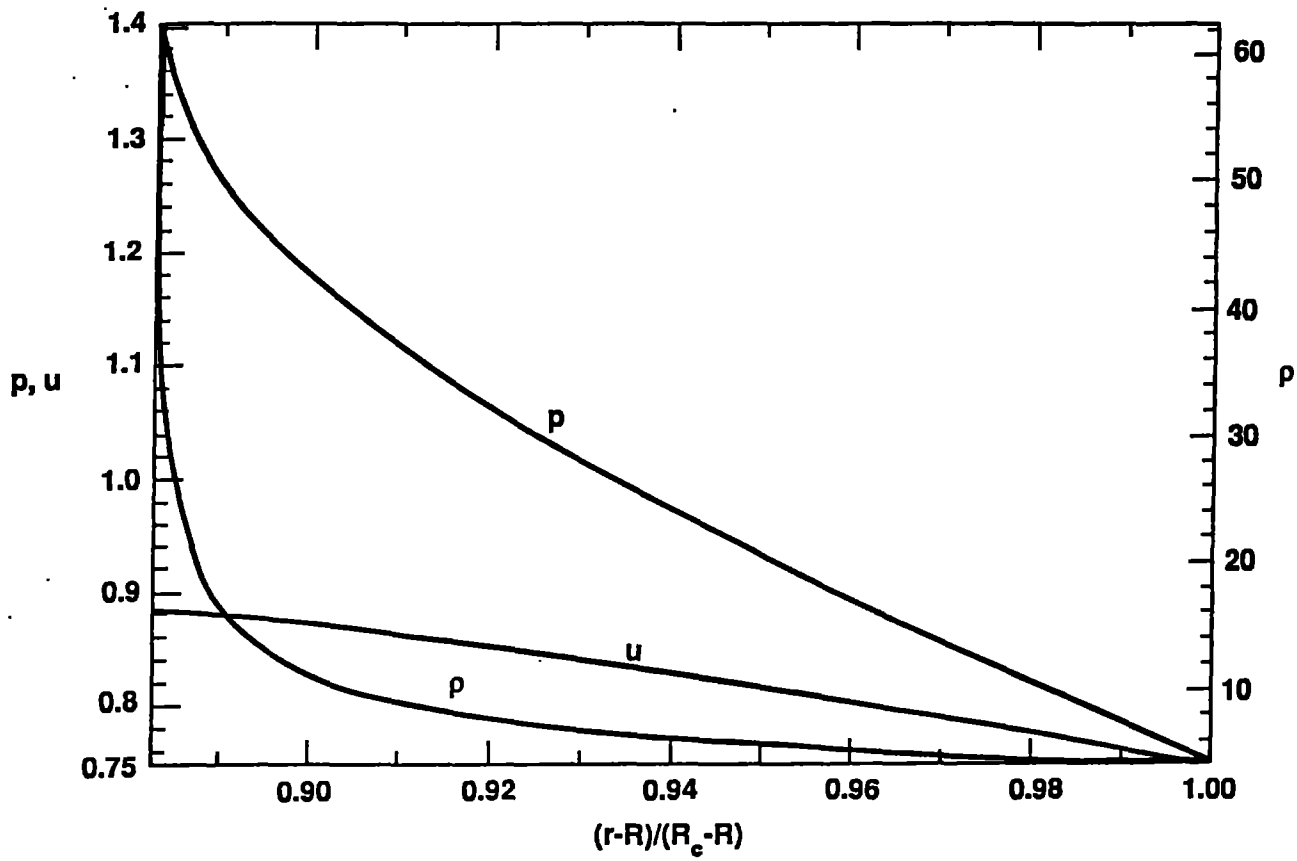
1.4
1.3
1.2
1.1
1.0
0.9
0.8
0.75
p, u
60
50
40
30
20
10
ρ
p
u
ρ
0.90
0.92
0.94
0.96
0.98
1.00
(r-R)/(R_c-R)

Fig. 2